© 2018. Published by The Company of Biologists Ltd | Development (2018) 145, dev159400. doi:10.1242/dev.159400

RESEARCH REPORT

Commissural neurons transgress the CNS/PNS boundary in absence of ventricular zone-derived netrin 1

Juan Antonio Moreno-Bravo[1,*], Sergi Roig Puiggros[1,*], Heike Blockus[1], Chloé Dominici[1], Pavol Zelina[1], Patrick Mehlen[2] and Alain Chédotal[1,‡]

ABSTRACT

During the development of the central nervous system (CNS), only motor axons project into peripheral nerves. Little is known about the cellular and molecular mechanisms that control the development of a boundary at the CNS surface and prevent CNS neuron emigration from the neural tube. It has previously been shown that a subset of spinal cord commissural axons abnormally invades sensory nerves in *Ntn1* hypomorphic embryos and *Dcc* knockouts. However, whether netrin 1 also plays a similar role in the brain is unknown. In the hindbrain, precerebellar neurons migrate tangentially under the pial surface, and their ventral migration is guided by netrin 1. Here, we show that pontine neurons and inferior olivary neurons, two types of precerebellar neurons, are not confined to the CNS in *Ntn1* and *Dcc* mutant mice, but that they invade the trigeminal, auditory and vagus nerves. Using a *Ntn1* conditional knockout, we show that netrin 1, which is released at the pial surface by ventricular zone progenitors is responsible for the CNS confinement of precerebellar neurons. We propose, that netrin 1 distribution sculpts the CNS boundary by keeping CNS neurons in netrin 1-rich domains.

KEY WORDS: Netrin, Dcc, Pontine neurons, Cerebellum, Migration, Commissural neurons

INTRODUCTION

Netrin 1 is a secreted protein that controls cell-cell interactions in many organs and species, during development and in pathological conditions (Mehlen et al., 2011). In the central nervous system (CNS), netrin 1 promotes axon outgrowth to the midline, axon attachment to their targets and neuronal migration (Akin and Zipursky, 2016; Serafini et al., 1994, 1996; Yee et al., 1999). Netrin 1 is secreted, but acts locally by promoting cell adhesion and haptotaxis (Akin and Zipursky, 2016; Li et al., 2004; Moore et al., 2009). In the mouse hindbrain and spinal cord, netrin 1 is not only produced by the floor plate, but is also released at the pial surface by neural precursors of the ventricular zone (Dominici et al., 2017; Kennedy et al., 1994; Varadarajan et al., 2017). This suggests that netrin 1 accumulation in the basal lamina provides a permissive substrate for axon extension. In the spinal cord, netrin 1 and its receptor deleted in colorectal cancer (Dcc) influence the confinement of commissural axons to the CNS (Laumonnerie et al., 2014). In the spinal cord, two repulsive guidance cues, netrin 5 and Sema6A, also act as gate keepers at the CNS/PNS border (Bron et al., 2007; Garrett et al., 2016; Mauti et al., 2007). Both cues are expressed by so-called boundary cap (BC) cells, which constrain motor neurons and oligodendrocyte soma to the spinal cord and prevent them from migrating along motor nerves into the PNS (Kucenas et al., 2009; Vermeren et al., 2003). Whether such mechanisms are at play at the level of the hindbrain is unknown.

Interestingly, several classes of hindbrain neurons preferentially migrate tangentially under the pial surface in a netrin 1-rich domain (Stanco and Anton, 2013). This occurs in the case of the pontine nucleus, one of the four hindbrain precerebellar nuclei that contain neurons projecting to the cerebellum. Pontine neurons are born in the rhombic lip, a dorsal neuroepithelium that lines the fourth ventricle (Wullimann, 2011). Pontine neurons form a compact and superficial migratory stream that first progresses anteriorly before turning ventrally towards the floor plate (Geisen et al., 2008; Kratochwil et al., 2017; Zelina et al., 2014). Pontine neurons fail to migrate ventrally in *Ntn1* hypomorphic mutants and their number is reduced (Yee et al., 1999; Zelina et al., 2014). Here, we show that netrin 1, acting at least in part through the Dcc receptor, prevents pontine neurons and other classes of hindbrain commissural neurons from exiting the CNS through sensory nerve roots.

RESULTS

A few commissural axons project outside the spinal cord in netrin 1 hypomorph embryos ($Ntn1^{\beta geo/\beta geo}$) (Laumonnerie et al., 2014). We first confirmed this observation using immunostaining for Robo3, a marker of commissural neurons (Friocourt and Chédotal, 2017; Sabatier et al., 2004) on E11 embryos (Fig. 1A-L). To facilitate the analysis, whole-mount immunostaining was performed followed by 3DISCO clearing and three-dimensional (3D) imaging with light-sheet fluorescence microscopy (LSFM) (Belle et al., 2014). In $Ntn1^{\beta geo/+}$ embryos, Robo3$^+$ axons were restricted to the spinal cord, extending dorso-ventrally and crossing the midline (Fig. 1A,D, Fig. S1A,B, Movie 1), whereas in $Ntn1^{\beta geo/\beta geo}$ embryos, Robo3$^+$ axons were also seen outside the spinal cord, within dorsal root ganglia (DRG) labeled with anti-islet 1 (Fig. 1B,E and Fig. S1C,D). A few Robo3$^+$ axons were also seen in the ventral roots (data not shown). Next, we studied a null allele of *Ntn1* (see Materials and Methods), $Ntn1^{-/-}$. Robo3$^+$ axons also left the spinal cord in $Ntn1^{-/-}$ embryos (Fig. 1C,F, Fig. S1E,F and Movie 2). Importantly, unlike in control embryos (Fig. 1G,H), Robo3$^+$ axons were detected outside the CNS in the hindbrain, both in $Ntn1^{\beta geo/\beta geo}$ embryos (Fig. 1I,J) and $Ntn1^{-/-}$ embryos (Fig. 1K,L). As in the spinal cord, commissural axons escaped the CNS via sensory roots and this was particularly striking at the trigeminal and vestibular nerve roots (Fig. 1K,L and

[1]Sorbonne Universités, UPMC Université Paris 06, INSERM, CNRS, Institut de la Vision, 75012 Paris, France. [2]Apoptosis, Cancer and Development Laboratory, Equipe labellisée 'La Ligue', LabEx DEVweCAN, Centre de Recherche en Cancérologie de Lyon, INSERM U1052-CNRS UMR5286, Université de Lyon, Centre Léon Bérard, 69008 Lyon, France.
*These authors contributed equally to this work

‡Author for correspondence (alain.chedotal@inserm.fr)

A.C., 0000-0001-7577-3794

Received 14 September 2017; Accepted 12 December 2017

Development (2018) 145, dev159400. doi:10.1242/dev.159400

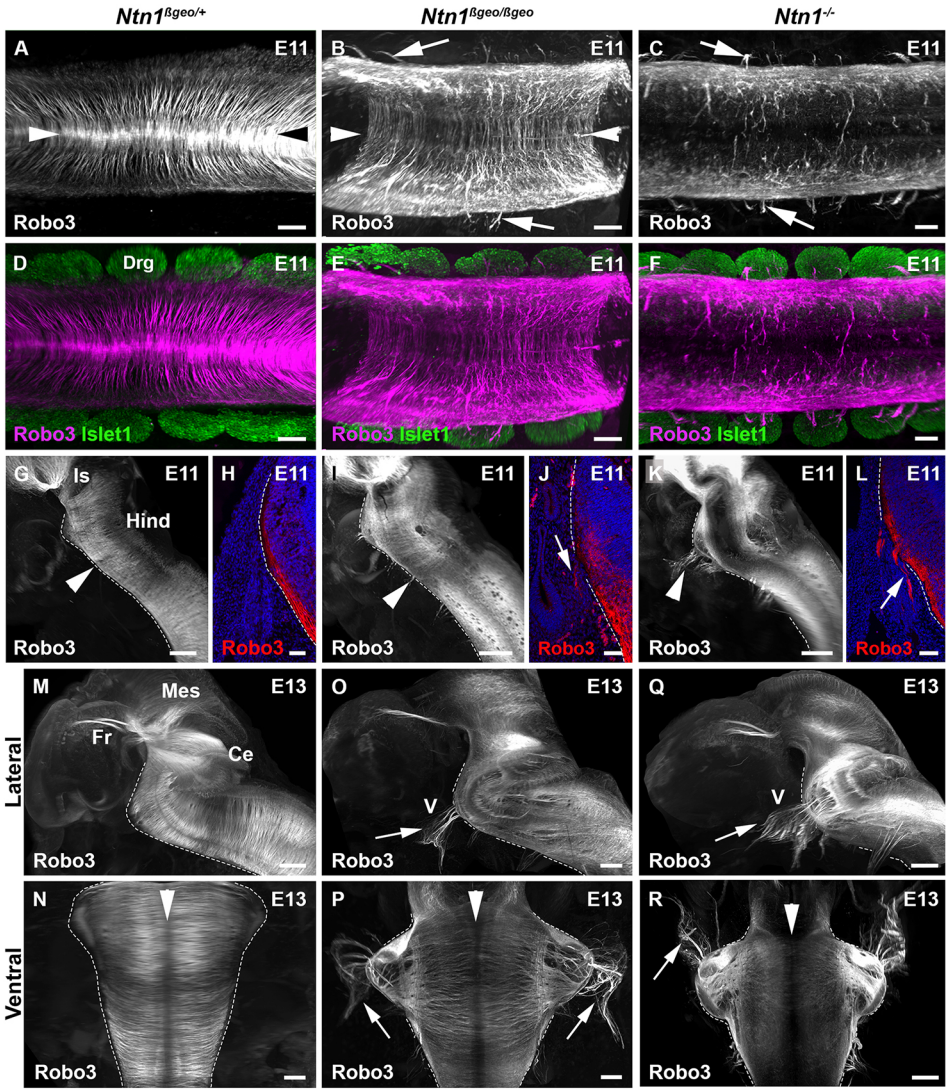

Fig. 1. Netrin 1 prevents commissural axon exit from the central nervous system. (A-F) Light-sheet fluorescence microscopy images of the spinal cord of E11 embryos immunolabeled for Robo3 and islet 1. In wild type (A,D; *n*=3), commissural axons extend dorsoventrally towards the floor plate (arrowheads in A), and are absent from islet1$^+$ dorsal root ganglia (Drg) (D). In *Ntn1*$^{ßgeo/ßgeo}$ (B,E; *n*=5) and *Ntn1*$^{-/-}$ (C,F; *n*=6) mutants, some Robo3$^+$ commissural neurons exit the spinal cord and invade dorsal root ganglia (arrows in B and C). Arrowheads in B indicate the floor plate. (G,H) In wild-type E11 hindbrain, Robo3$^+$ axons are also confined to the CNS (arrowhead in G, *n*=5). (I-L) In *Ntn1*$^{ßgeo/ßgeo}$ (I,J; *n*=4) and *Ntn1*$^{-/-}$ (K,L; *n*=6) mutants, Robo3$^+$ axons exit the CNS via sensory roots (arrowheads in I,K; arrows in J, L). (M-R) At E13, hindbrain commissural axons still express Robo3 (M,N; *n*=5). In *Ntn1*$^{ßgeo/ßgeo}$ (O,P; *n*=4) and *Ntn1*$^{-/-}$ (Q,R; *n*=6) knockouts, commissural axons invade the trigeminal nerve (V; arrows in O-R). The arrowheads in N,P,R indicate the ventral midline. Ce, cerebellum; Hind, hindbrain; Is, isthmus; Mes, mesencephalon; Fr; fasciculus retroflexus. Scale bars: 100 µm in A-F; 300 µm in G,I,K; 50 µm in H,J,L; 400 µm in M-R.

Fig. S1G-J). The amount of Robo3$^+$ axons invading the PNS at the hindbrain level was significantly lower in *Ntn1*$^{βgeo/βgeo}$ compared with the *Ntn1*$^{-/-}$ embryos (Fig. S1S and Table S1).

In the hindbrain, commissural neurons are produced at least until E16 (Pierce, 1966; Zelina et al., 2014). Therefore, we next studied *Ntn1* mutant embryos at E13 and E16. In control embryos, Robo3 axons were only found in the CNS (Fig. 1M,N and Movie 3), whereas in *Ntn1*$^{βgeo/βgeo}$ embryos and *Ntn1*$^{-/-}$ embryos, Robo3$^+$ axons massively invaded trigeminal and vestibular nerves and ganglia (Fig. 1O-R and Movie 4). This defect was more pronounced in *Ntn1*$^{-/-}$ than in *Ntn1*$^{βgeo/βgeo}$ mutants (Fig. S1T and Table S1). At E16, only pontine neurons still express Robo3 in the hindbrain of control embryos (Fig. 2A-C and Movie 5) (Marillat et al., 2004; Zelina et al., 2014), suggesting that some of the Robo3$^+$ axons leaving the brain in *Ntn1*$^{βgeo/βgeo}$ (Fig. 2D-F) and *Ntn1*$^{-/-}$ (Fig. 2G-I) E16 embryos could belong to pontine neurons. This hypothesis was tested using immunostaining for Barhl1 and Pax6, two markers of migrating pontine neurons (Benzing et al., 2011; Zelina et al., 2014). In controls, the auditory and trigeminal nerves and ganglia did not contain Barhl1$^+$/Robo3$^+$ or Pax6$^+$ neurons (Fig. 2A-C,J-N and Fig. S1K,L,O,P). By contrast, streams of Barhl1$^+$/Robo3$^+$ or Pax6$^+$/Robo3$^+$ cells were seen inside these nerves in *Ntn1*$^{βgeo/βgeo}$ (Fig. 2O-S and Fig. S1M,Q) and *Ntn1*$^{-/-}$ embryos (Fig. 2T-X, Fig. S1N,R and Movie 6), that could be traced back to the pontine migratory stream in the hindbrain (Fig. 2D-I). In wild-type embryos, Barhl1$^+$/Robo3$^+$ neurons are absent from trigeminal and vestibular ganglia, which contains Sox10$^+$ sensory neurons (Fig. 2J-N). By contrast, there was a significant colonization of trigeminal and vestibular nerves and ganglia by streams and clusters of Barhl1$^+$ neurons in *Ntn1*$^{βgeo/βgeo}$ embryos and *Ntn1*$^{-/-}$ embryos (Fig. 2O-X and Fig. S1U and Table S2). Ectopic Barhl1$^+$ neurons were not immunoreactive for Sox10 (Fig. 2P,Q,U,V) but expressed Robo3 (Fig. 2R,S,W,X), supporting their pontine neuron identity.

To confirm that these neurons originated from the CNS, we electroporated a plasmid encoding green fluorescent protein (GFP) into the rhombic lip of *Ntn1*$^{-/-}$ E13.5 embryos (*n*=4) and collected them at E16. This selectively drives GFP expression in migrating pontine neurons (Kawauchi, 2006; Zelina et al., 2014). In all controls (*n*=10), GFP$^+$ neurons were restricted to the hindbrain (Fig. 2Y), whereas in all *Ntn1*$^{-/-}$ embryos (Fig. 2Z,Z′ and Movie 7), many GFP$^+$/Robo3$^+$ processes and cell bodies were found within the auditory and trigeminal nerves. Together, these data show that neurons maintaining a pontine identity transgress the PNS/CNS boundary in absence of netrin 1 and migrate along nerve roots. Their long-term fate could not be assessed as both types of *Ntn1* mutants die at birth.

Development (2018) 145, dev159400. doi:10.1242/dev.159400

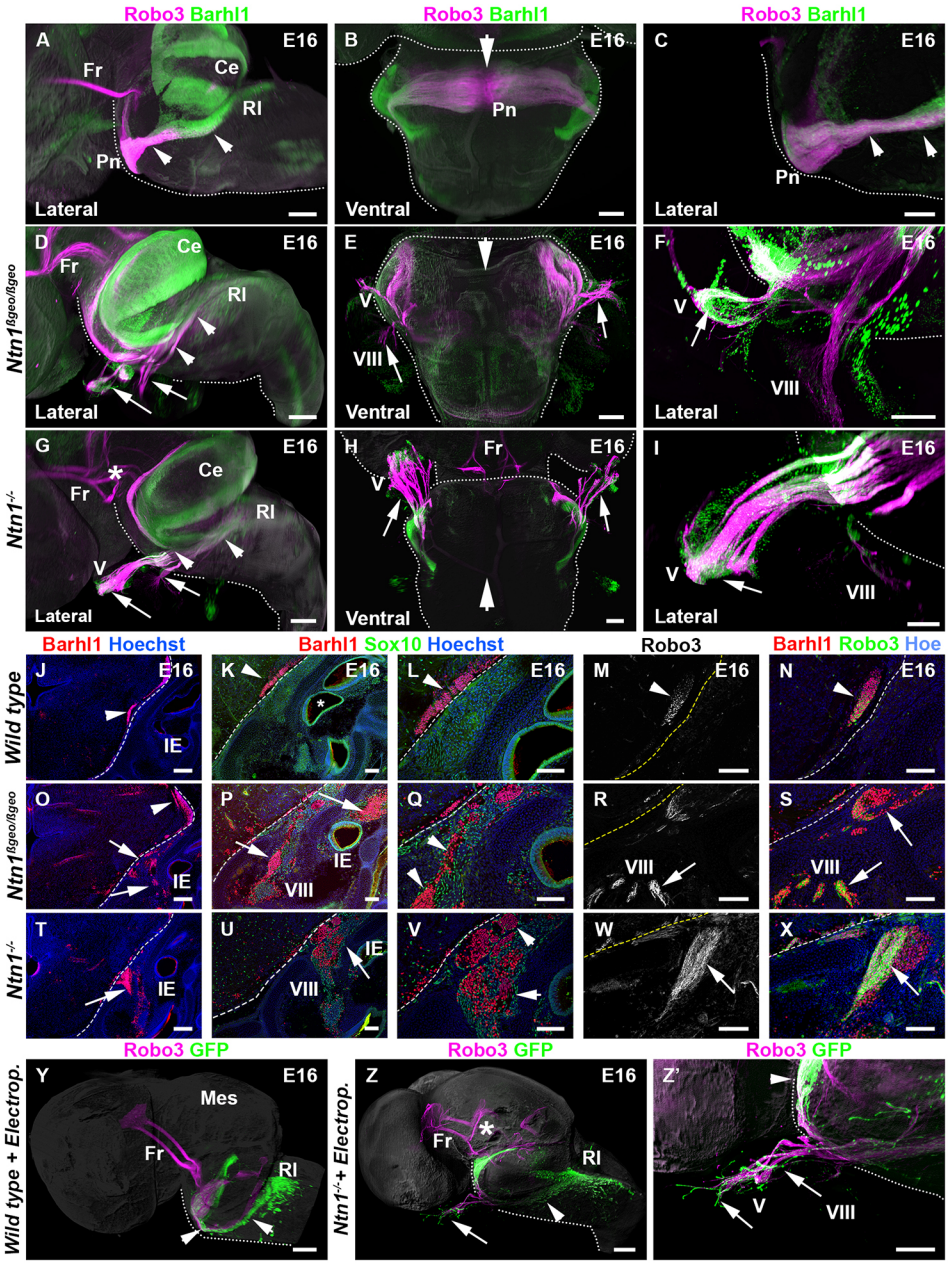

Fig. 2. Migrating pontine neurons invade the peripheral nervous system in the absence of netrin 1. (A-I) 3D light-sheet fluorescence microscopy images of whole-mount E16 embryos labeled with anti-Robo3 (magenta) and anti-Barhl1 (green) antibodies. (A-C) In wild type, pontine neurons (Pn) leave the rhombic lip dorsally (Rl) and migrate under the pial surface (dotted line) to the floor plate (arrowhead in B) along the anterior extramural stream (arrowheads in A and C; *n*=6). (D-I) In *Ntn1*$^{ßgeo/ßgeo}$ (D-F; *n*=5) and *Ntn1*$^{-/-}$ (G-I; *n*=5) mutants, pontine neurons leave the rhombic lip (arrowheads in D and G), but neuronal chains exit the CNS by the auditory (VIII and short arrow) and trigeminal (V) nerves (arrow). Pontine neurons fail to reach the midline in the absence of netrin 1 (arrowheads in E and H). The asterisk in G indicates the abnormal fasciculus retroflexus (Fr). (J-X) E16 hindbrain cryosections. In wild type (J-N; *n*=5), Barhl1^{+} pontine neurons are confined to the CNS (arrowheads in J-L) and express Robo3 (arrowhead in N). Arrowhead in M indicates pontine neurons. Barhl1^{+} cells are not immunoreactive for Sox10, a neural crest cell and dorsal root ganglion neuron marker (K, L; *n*=5). In *Ntn1* mutants (O-X), a fraction of Barhl1^{+}/Robo3^{+} Pn neurons (arrows) migrate into the trigeminal (V) and auditory nerves, and reach the inner ear (IE). These cells do not express Sox10 [arrowheads in Q (*n*=4) and V (*n*=5)]. Arrowhead in O indicates pontine neurons in the CNS. (Y-Z′) Light-sheet fluorescence microscopy images of E16 embryos electroporated at E13 with GFP. Whole-mount GFP and Robo3 immunostaining and 3DISCO clearing. In wild type (Y; *n*=10), GFP^{+} PN neurons (arrowheads) are restricted to the CNS migrating from the rhombic lip (Rl) to the midline. In all *Ntn1*$^{-/-}$ mutants (Z and Z′; *n*=4), Robo3^{+} and GFP^{+} neurons migrate from the rhombic lip (arrowhead in Z) but some exit the CNS and invade the trigeminal nerve (arrows in Z′). Asterisk in Z indicates the abnormal fasciculus retroflexus. Ce, cerebellum; Mes, mesencephalon; Fr; fasciculus retroflexus. Dotted lines represent the CNS limit. Scale bars: 300 µm in B,C,E,F,H, I,J-X; 500 µm in A,D,G,Y,Z,Z′.

Netrin 1 has either growth-promoting or growth-inhibiting activity and could act as a repulsive barrier at sensory nerve roots. However, *Ntn1* mRNA was absent from DRG and hindbrain sensory ganglia (Fig. S2A,C) and was only found in the floor plate, ventricular zone progenitors and cochlea, as previously described (Abraira et al., 2008; Dominici et al., 2017; Laumonnerie et al., 2014; Serafini et al., 1994). These results were confirmed by monitoring β-galactosidase and netrin 1 protein expression in *Ntn1*$^{ßgeo/+}$ E13 embryos (Fig. S2B,D). β-Gal was present in floor plate and ventricular zone precursors, and netrin 1 accumulated at the pial surface, as recently described (Dominici et al., 2017; Varadarajan et al., 2017). It was also detected in the inner ear (Nishitani et al., 2017) and in some mesenchymal cells but not in sensory ganglia. Netrin 1 levels were high in nestin^{+} radial glia endfeet but stopped dorsally at the level of the vestibular and trigeminal nerve roots (Fig. S2E,F). Netrin 1 staining was abrogated in *Ntn1*$^{-/-}$ embryo but nestin^{+} glial endfeet were organized normally as previously described (Fig. S2G,H) (Dominici et al., 2017). Importantly, netrin 1 and β-gal were absent from commissural neurons, including migrating pontine neurons. The absence of netrin 1 in sensory ganglia and nerves suggests that it is unlikely to act as a repulsive barrier.

To further characterize netrin 1 function at the CNS/PNS boundary, we next performed selective genetic ablation of netrin 1 from various cellular sources using specific Cre-recombinase driver lines and a *Ntn1* conditional allele (*Ntn1*$^{fl/fl}$) (Dominici et al., 2017). Cre expression was confirmed using a *Rosa*^{tdTomato} reporter line (Fig. S2I-L). As in *Ntn1*$^{fl/+}$ (Fig. 3A-C), no Robo3^{+} axons were detected in the PNS of *Shh:Cre;Ntn1*$^{fl/fl}$ E13 embryos (Fig. 3D-F), which completely lack netrin 1 at the floor plate (Dominici et al., 2017) (Fig. S2I). Next, we studied *Nes:Cre;Ntn1*$^{fl/fl}$ E13 embryos in which netrin 1 is deleted from neural cells in the CNS and PNS but maintained in floor plate and inner ear (Fig. S2K) (Dominici et al., 2017). Interestingly, a massive invasion of peripheral nerve roots by

Development (2018) 145, dev159400. doi:10.1242/dev.159400

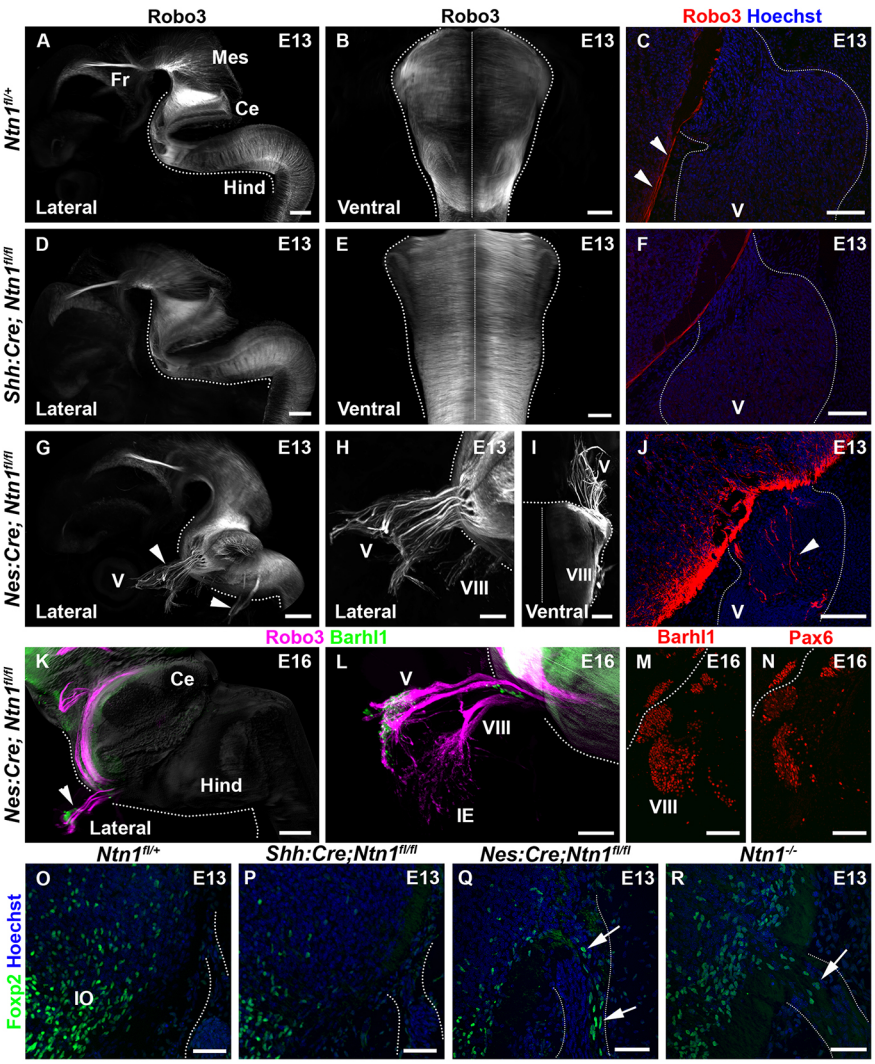

Fig. 3. Ventricular zone-derived netrin 1 is required for commissural axons and precerebellar neuron CNS confinement. (A-C) At E13, Robo3^{+} hindbrain commissural axons extend below the CNS/PNS boundary (arrowheads in C) to the ventral midline (A,B; *n*=5). (D-F) This is also the case in *Shh:Cre; Ntn1$^{fl/fl}$* mutants, which lack netrin 1 in floor plate (*n*=6). (G-J) In *Nes:Cre;Ntn1$^{fl/fl}$* mutants, which lack ventricular zone-derived netrin 1, Robo3^{+} commissural axons escape from the hindbrain through sensory ganglia, including the trigeminal (V; arrowheads in G,J, *n*=5). (K-N) In *Nes:Cre;Ntn1$^{fl/fl}$* E16 embryos, pontine neurons invade the trigeminal (V) and auditory (VIII and arrowhead in K) nerves. (M,N) Hindbrain cryosections showing Barhl1- (M) and Pax6- (N) immunopositive cell bodies in the auditory nerve. Dotted lines in the panels indicate the CNS limit (*n*=5). (O-R) Coronal sections of E13 embryos immunolabeled for Foxp2, an inferior olivary (IO) neuron marker. The dotted line delineates the vagus nerve. In wild-type (O, *n*=6) and *Shh:Cre; Ntn1$^{fl/fl}$* (P; *n*=4) embryos, Foxp2^{+} IO neurons migrate only within the CNS. By contrast, a subset of Foxp2^{+} cells leave the CNS (arrows) to enter the vagus nerve in *Nes:Cre;Ntn1$^{fl/fl}$* (Q; *n*=4) and *Ntn1$^{-/-}$* mutants (R; *n*=4). Ce, cerebellum; Fr, fasciculus retroflexus; Hind, hindbrain; Mes, mesencephalon. Scale bars: 300 µm in A,D,G; 150 µm in B,E,H,L; 100 µm in C,F,J,M,N; 200 µm in I; 500 µm in K; 50 µm in O-R.

commissural axons was seen in *Nes:Cre;Ntn1$^{fl/fl}$* E13 embryos, with Robo3^{+} axons extending far in the trigeminal nerve branches and in the vestibular nerve (Fig. 3G-J). The phenotype was as severe as in *Ntn1$^{-/-}$* and *Ntn1$^{\beta geo/\beta geo}$* mutants (Fig. S1T and Table S1). At E16, streams of Barhl1^{+}/Robo3^{+} and Pax6^{+} pontine neurons were also detected within the trigeminal and auditory nerves (Fig. 3K-N, Fig. S1U and Table S2). Interestingly, a subset of Foxp2^{+} cells, most likely corresponding to inferior olivary neurons (Dominici et al., 2017), also escaped the CNS in *Nes:Cre;Ntn1$^{fl/fl}$* and *Ntn1$^{-/-}$* E13 embryos to enter the vagus nerve (Fig. 3O-R). Together, these data show that a massive exit of hindbrain commissural neurons from the CNS is caused by the absence of netrin 1 from CNS cells.

Boundary cap (BC) cells might prevent commissural neuron from escaping the CNS as they do for motor neurons. To visualize BC cells in control and *Ntn1* mutant embryos, we performed *in situ* hybridization for *Prss56*, which encodes a potentially secreted trypsin-like serine protease highly expressed by BC cells (Coulpier et al., 2009). Prss56^{+} BC cells were found at the level of all nerve roots in the spinal cord and hindbrain both in wild-type E11 and E13 embryos (Fig. S2M,N,Q,R) but also in *Ntn1$^{-/-}$* mutant embryos (Fig. S2O,P,S,T). This shows that the invasion of the PNS by commissural neurons is not due to a lack of BC cells.

Netrin 1 has several receptors, including Dcc and Unc5s (Unc5a-d) (Ackerman et al., 1997; Kolodziej et al., 1996). It has previously been shown that commissural axons also enter the DRGs in Dcc knockouts but not in Unc5a/Unc5c knockouts (Laumonnerie et al., 2014). We could confirm this result using whole-mount immunolabeling for Robo3 on E11 *Dcc$^{-/-}$* embryos. As in *Ntn1* mutants, Robo3^{+} axons were detected within the trigeminal and vestibular nerves at E11 (Fig. 4A, Table S3), E13 (Fig. 4B-D, Table S3) and E16 (Fig. 4E). Some were pontine neurons, as shown with Pax6/Barhl1 immunolabeling (Fig. 4E-F). A similar defect was seen in a second *Dcc* null allele, *Dcc$^{\Delta/\Delta}$*, resulting from the intercross of *Dcc$^{fl/fl}$* mice to a line expressing cre in the germline (see Materials and Methods; Fig. 4G). To determine whether Dcc acts in pontine neurons to constrain their migration to the CNS, we next crossed the *Dcc$^{fl/fl}$* mice to *Wnt1:Cre* line (Danielian et al., 1998; Zelina et al., 2014). As in *Dcc$^{-/-}$* embryos, pontine neurons were unable to migrate towards the floor plate in *Dcc$^{\Delta/\Delta}$* and *Wnt1:Cre;Dcc$^{fl/fl}$* E16 embryos (Zelina et al., 2014 and data not shown). In addition, Robo3^{+} axons and Barhl1^{+}/Pax6^{+} neurons were found in the trigeminal and vestibular ganglia of *Wnt1:Cre;Dcc$^{fl/fl}$* E16 embryos (Fig. 4H-K,L), indicating that a the lack of Dcc in pontine neurons induces some of them to exit the CNS (Fig. 4M).

Development (2018) 145, dev159400. doi:10.1242/dev.159400

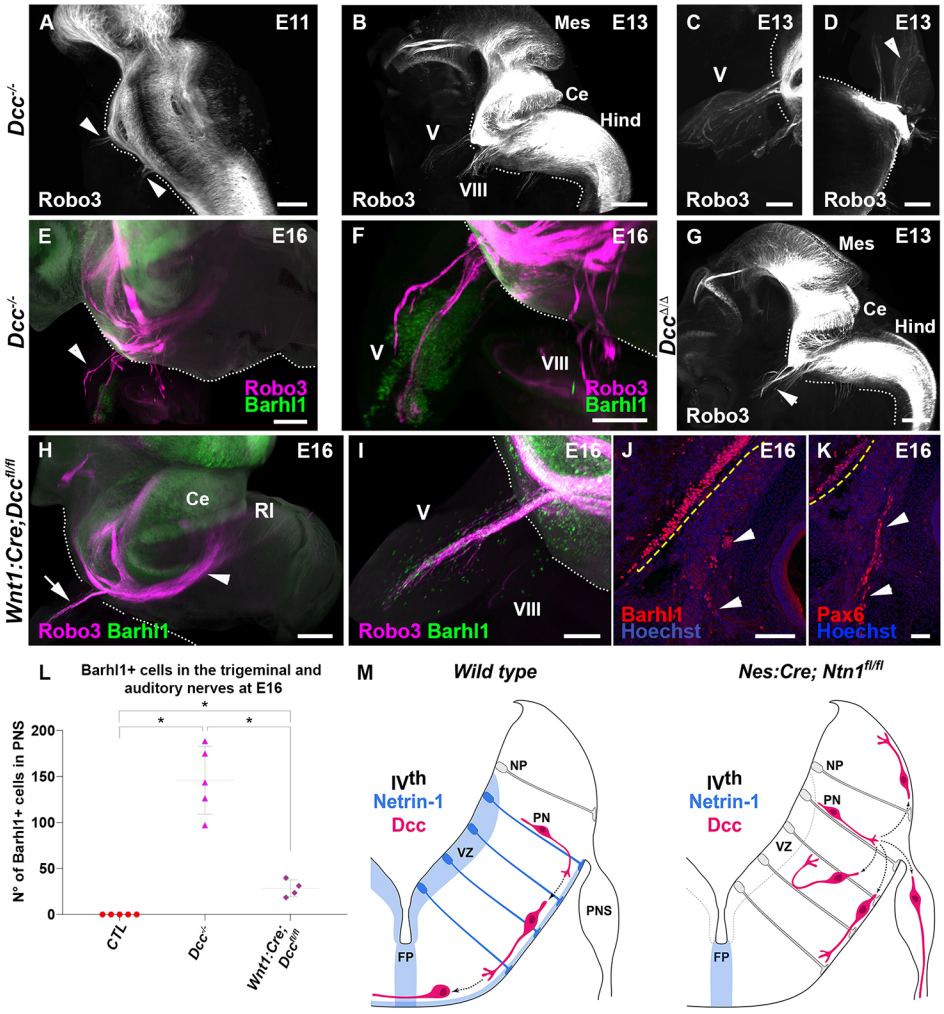

Fig. 4. The CNS confinement of commissural neurons involves Dcc. (A-I) Light-sheet fluorescence microscopy images of 3DISCO-cleared embryos. (A-F) In E11 (A, *n*=4) and E13 (B-D; *n*=4) $Dcc^{-/-}$ mutants, some Robo3^{+} commissural axons exit the CNS through nerve roots (arrowheads in A), including the trigeminal (V and arrowhead in D) and auditory (VIII) nerves. At E16, Barhl1^{+}/Robo3^{+} pontine neurons enter the trigeminal nerve (arrowheads in E, *n*=3). (G) The invasion of the PNS by Robo3^{+} axons (arrowhead) is also observed in E13 $Dcc^{\Delta/\Delta}$ mutants (*n*=3). (H-K) In *Wnt1:Cre;*$Dcc^{fl/fl}$ mutants, a stream of Robo3^{+}/Barhl1^{+} pontine neurons migrates from the rhombic lip (Rl, arrow) but some enter the trigeminal nerve (arrowhead in H). (J,K) Coronal sections showing the presence in the PNS of Barhl1^{+} and Pax6^{+} pontine neurons in the inner ear (arrowheads, *n*=4). (L) Quantification of the number of Barhl1^{+} cells in the auditory and trigeminal nerves in control, $Dcc^{-/-}$ and *Wnt1:Cre;* $Dcc^{fl/fl}$ E16 cryosections (see Table S4). (M) Schematic representations of precerebellar neuron migration in control and Ntn1-deficient mice. Ce, cerebellum; Hind, hindbrain; PN, precerebellar neuron; NP, neural precursor; VZ, ventricular zone; FP, floor plate; PNS, peripheral nervous system. Dotted lines in the panels represent the CNS limit. Scale bars: 400 µm in A,B,E-H; 200 µm in C,D,I; 100 µm in J; 50 µm in K.

DISCUSSION

At early developmental stages, neural crest cells migrate out of the neural tube to colonize the embryo to form most of the PNS and a variety of tissue and organs. However, after neural crest cell migration is completed, the PNS and the CNS segregate and newly born CNS cells remain confined to the CNS. Sensory axons from the PNS can still enter the CNS but at specific locations (such as the dorsal root entry zone in the spinal cord). In the CNS, motor axons will cross the CNS/PNS boundary to project to their target muscles, but boundary cap cells prevent motor neurons from entering the nerves. *In vitro* evidence also suggest that meninges might also control the CNS/PNS border (Suter et al., 2017). However, the cellular and molecular mechanisms that shape the CNS/PNS interface are not well characterized. Here we show that netrin 1, which is secreted at the CNS basal lamina by neural precursor endfeet, prevents various populations of hindbrain commissural neurons, in particular pontine neurons, from migrating into the PNS through nerve roots. In the spinal cord and in the hindbrain, a subset of commissural axons is misguided from early developmental stages and project into nerve roots. Therefore, it is possible that these first escapers lead the way for later-born commissural neurons in particular precerebellar neurons that migrate close to the pial surface and in the vicinity of trigeminal and auditory nerve roots. We propose that commissural neurons do not actively avoid nerve roots in a repulsive manner, but that they preferentially extend on netrin 1, which appears largely absent from the nerve roots. Without netrin 1, the growth of commissural axons and the migration of pontine neurons is more erratic and randomized, and they can invade the nerve roots. Although motor neurons express Dcc, like commissural axons, their axons can extend into the PNS. However, it has previously been shown that Dcc is inactive in motor neurons as it is cleaved by presenilin, and that they are unresponsive to netrin 1 within the spinal cord (Bai et al., 2011).

Interestingly, during normal development pontine neurons exhibit features of so-called collective migration, previously described for neural crest cells and lateral line neurons, among others (Friedl and Mayor, 2017). Pontine neurons migrate along each other in a compact stream from the rhombic lip to the floor plate. We show that, in the absence of netrin 1, pontine neuron cohesion appears affected and some escape from the main stream to invade the nerve roots. This suggests that netrin 1 might control collective cell migration in this system. Our results suggest that Dcc mediates netrin 1 function at the CNS/PNS boundary. However, the milder pontine neuron emigration defects observed in *Dcc* KO compared with *Ntn1* KO indicate that another receptor, such as the Dcc paralogue neogenin (Keino-Masu et al., 1996) could also contribute. Unc5 receptors are unlikely to be involved, as pontine neurons remain in the CNS in Unc5b and Unc5c knockouts (Di Meglio et al., 2013; Kim and Ackerman, 2011). Together, our

Development (2018) 145, dev159400. doi:10.1242/dev.159400

results reveal a novel molecular mechanism controling the establishment of the CNS/PNS boundary (Fig. 4M).

MATERIALS AND METHODS

Mouse strains and genotyping

Ntn1$^{\beta geo}$ (Serafini et al., 1996) and *Dcc* (Fazeli et al., 1997) knockout lines have been previously described and genotyped by PCR. The *Ntn1* conditional knockout and the *Ntn1*-null allele were generated as described elsewhere (Dominici et al., 2017). To generate a null allele of Dcc, *Dcc*$^{fl/fl}$ mice (Krimpenfort et al., 2012) were crossed to *Krox20:Cre* mice, which express Cre recombinase in both male and female germlines after sexual maturity (Voiculescu et al., 2000).

To ablate netrin 1 and Dcc expression from their different sources, we used different Cre lines: for the floor plate cells we used the *Shh:Cre* line (Harfe et al., 2004) (Jackson Laboratories); for the ventricular zone precursors we used the *Nestin:Cre* line (Tronche et al., 1999); and, finally, for the rhombic lip derivatives (pontine neurons), we used the *Wnt1:Cre* line (Danielian et al., 1998). The Ai9 *Rosa*^{tdTomato} reporter line (*Rosa*^{Tom}; Jackson Laboratories) was used to analyze the Cre expression driven by the different lines. All mice were kept in C57BL/6 background and the day of females vaginal plug was counted as embryonic day 0.5 (E0.5). Mice were anesthetized with ketamine (100 mg/ml) and xylazine (10 mg/ml). All animal procedures were carried out in accordance to institutional guidelines and approved by the UPMC University ethic committee (Charles Darwin). Embryos of either sex were used.

In situ hybridization

Antisense RNA probes were labeled with digoxigenin-11-d-UTP (Roche Diagnostics) as described elsewhere (Marillat et al., 2004), by *in vitro* transcription of cDNA encoding mouse *Ntn1* (Serafini et al., 1996), mouse *Ntn1 exon 3* (Dominici et al., 2017) and mouse *Prss56* (Coulpier et al., 2009).

Immunohistochemistry

Fixation was performed by embryo immersion in 4% paraformaldehyde in 0.12 M phosphate buffer (pH 7.4) (PFA) overnight at 4°C. Samples were cryoprotected in a solution of 10% sucrose, for E11 and E13 embryos, and 30% sucrose for E16 embryos, in 0.12 M phosphate buffer (pH 7.2), frozen in isopentane at −50°C. Immunohistochemistry was performed on cryostat sections (20 µm) after blocking in 0.2% gelatin in PBS containing 0.25% Triton-X100 (Sigma). Sections were then incubated overnight at room temperature with the following primary antibodies: goat anti-human Robo3 (1:250, R&D Systems, AF3076), goat anti-Dcc (1:500, Santa Cruz, sc-6535), rat anti-mouse netrin 1 (1:500, R&D Systems, MAB1109), mouse anti-Nestin-Alexa488 (1:1000, Abcam, ab197495), rabbit anti-β-gal (1:500, Cappel, 55976), rabbit anti-Dsred (1:500, Clontech, 632496), rabbit anti-Pax6 (1:500, Millipore, AB2237), rabbit anti-Barhl1 (1:500, Sigma, HPA004809), rabbit anti-mouse Islet1 (1:500, Abcam, ab20670), anti-Sox10 (1:500, Santa Cruz, sc-17342), goat anti-FoxP2 (1:500, Santa Cruz, sc-21069) and rabbit anti-FoxP2 (1:500, Abcam, ab16046). Corresponding secondary antibodies directly conjugated to fluorophores (Cy-5, Cy-3, Alexa-Fluor 647 from Jackson ImmunoResearch, or from Invitrogen) were incubated during 2 h. For netrin 1 immunostaining, an antibody retrieval treatment was performed as described previously (Dominici et al., 2017). Sections were counterstained with Hoechst (1:1000, Sigma). Slides were scanned with a Nanozoomer (Hamamatsu) and laser scanning confocal microscope (FV1000, Olympus). Brightness and contrast were adjusted using Adobe Photoshop.

Whole-mount labeling, 3DISCO and methanol clearing

Whole-mount immunostaining and 3DISCO clearing procedures have been previously described (Belle et al., 2014, 2017). 3D imaging was performed with a light-sheet fluorescence microscope (Ultramicroscope I, LaVision BioTec) using Inspector Pro software (LaVision BioTec). Images and 3D volume were generated using Imaris ×64 software (Bitplane).

In utero electroporation

In utero electroporation of PN neurons was performed as described previously (Zelina et al., 2014), with some modifications. Endotoxin-free plasmid DNA of pCX-EGFP (1 µg/µl) (provided by Dr M. Okabe, Osaka University, Japan) alone was diluted in PBS containing 0.01% Fast Green. Diluted DNA (1 µl) was injected with a glass micropipette into the fourth ventricle of E13.5 mouse embryo. Five electric pulses (45 V, 50 ms, 950 ms interval between pulses) were applied with CUY21EDIT or NEPA21 electroporators (NepaGene) using 5 mm diameter electrodes (CUY650-5, Nepagene). Electroporated embryos were partially dissected at E16 followed by whole-mount labeling using goat anti-human Robo3 (1:250, R&D Systems AF3076) and chicken anti-GFP (1:1000, Abcam, ab13970).

Quantification and data analysis

Two different individuals, blinded to the experimental conditions, performed Robo3^{+} axon volume and Barhl1^{+} cell quantifications. There was no randomization in the groups and any statistical method was used to predetermine sample sizes. Graphical representations show mean values ±s.d. Statistical significance was measured using one-sided unpaired tests for non-parametric tendencies (Kruskal–Wallis and Mann–Whitney). For Robo3^{+} volume quantifications, a background subtraction was performed followed by 3D volumetric analysis, using Imaris ×64 software, to determine the total volume of Robo3^{+} fibers in the trigeminal nerve. The number of Barhl1^{+} cells in the auditory and trigeminal nerve roots was quantified within a rectangular area (340×380 µm) in five different sections. Two sections were taken at the auditory nerve root and three others at the trigeminal nerve root. Control embryos were from the same litters than the mutants. For both types of quantifications, at least four embryos of each genotype were quantified, from at least two different litters. In both quantifications, we considered differences to be significant when $P<0.05$ (see all statistical values in Tables S1-S4). All statistical analyses of the mean and variance were performed with Prism7 (GraphPad Software).

Acknowledgements

We thank Dr Piotr Topilko for providing the *Prss56* cDNA, Dr Marc Tessier-Lavigne for providing the *Ntn1βgeo* and Dcc knockouts, and Dr Anton Berns for providing the *Dcc* conditional knockout line.

Competing interests

The authors declare no competing or financial interests.

Author contributions

Conceptualization: J.A.M.-B., S.R.P., P.M., A.C.; Methodology: J.A.M.-B., S.R.P., H.B., P.Z., C.D., A.C.; Validation: A.C.; Formal analysis: J.A.M.-B., S.R.P., A.C.; Investigation: J.A.M.-B., A.C.; Resources: S.R.P., P.M., A.C.; Data curation: S.R.P., H.B., P.Z., C.D.; Writing - original draft: A.C.; Writing - review & editing: J.A.M.-B., S.R.P., H.B., P.Z., C.D., P.M.; Supervision: A.C.; Funding acquisition: A.C.

Funding

This work was supported by grants from the Agence Nationale de la Recherche (ANR-14-CE13-0004-01) (to A.C.). It was performed in the frame of the Labex Lifesenses (ANR-10-LABX-65) supported by French state funds managed by the Agence Nationale de la Recherche within the Investissements d'Avenir programme under ANR-11-IDEX-0004-02 (to A.C.).

Supplementary information

Supplementary information available online at
http://dev.biologists.org/lookup/doi/10.1242/dev.159400.supplemental

References

Abraira, V. E., del Rio, T., Tucker, A. F., Slonimsky, J., Keirnes, H. L. and Goodrich, L. V. (2008). Cross-repressive interactions between Lrig3 and netrin 1 shape the architecture of the inner ear. *Development* **135**, 4091-4099.

Ackerman, S. L., Kozak, L. P., Przyborski, S. A., Rund, L. A., Boyer, B. B. and Knowles, B. B. (1997). The mouse rostral cerebellar malformation gene encodes an UNC-5-like protein. *Nature* **386**, 838-842.

Akin, O. and Zipursky, S. L. (2016). Frazzled promotes growth cone attachment at the source of a Netrin gradient in the Drosophila visual system. *Elife* **5**, e20762.

Bai, G., Chivatakarn, O., Bonanomi, D., Lettieri, K., Franco, L., Xia, C., Stein, E., Ma, L., Lewcock, J. W. and Pfaff, S. L. (2011). Presenilin-dependent receptor processing is required for axon guidance. *Cell* **144**, 106-118.

Belle, M., Godefroy, D., Dominici, C., Heitz-Marchaland, C., Zelina, P., Hellal, F., Bradke, F. and Chédotal, A. (2014). A simple method for 3D analysis of immunolabeled axonal tracts in a transparent nervous system. *Cell Rep.* **9**, 1191-1201.

Belle, M., Godefroy, D., Couly, G., Malone, S. A., Collier, F., Giacobini, P. and Chédotal, A. (2017). Tridimensional visualization and analysis of early human development. *Cell* **169**, 161-173.e12.

Benzing, K., Flunkert, S., Schedl, A. and Engelkamp, D. (2011). A novel approach to selectively target neuronal subpopulations reveals genetic pathways that regulate tangential migration in the vertebrate hindbrain. *PLoS Genet.* **7**, e1002099.

Bron, R., Vermeren, M., Kokot, N., Andrews, W., Little, G. E., Mitchell, K. J. and Cohen, J. (2007). Boundary cap cells constrain spinal motor neuron somal migration at motor exit points by a semaphorin-plexin mechanism. *Neural Dev.* **2**, 21.

Coulpier, F., Le Crom, S., Maro, G. S., Manent, J., Giovannini, M., Maciorowski, Z., Fischer, A., Gessler, M., Charnay, P. and Topilko, P. (2009). Novel features of boundary cap cells revealed by the analysis of newly identified molecular markers. *Glia* **57**, 1450-1457.

Danielian, P. S., Muccino, D., Rowitch, D. H., Michael, S. K. and McMahon, A. P. (1998). Modification of gene activity in mouse embryos in utero by a tamoxifen-inducible form of Cre recombinase. *Curr. Biol.* **8**, 1323-13S2.

Di Meglio, T., Kratochwil, C. F., Vilain, N., Loche, A., Vitobello, A., Yonehara, K., Hrycaj, S. M., Roska, B., Peters, A. H. F. M., Eichmann, A. et al. (2013). Ezh2 orchestrates topographic migration and connectivity of mouse precerebellar neurons. *Science* **339**, 204-207.

Dominici, C., Moreno-Bravo, J. A., Roig Puiggros, S., Rappeneau, Q., Rama, N., Vieugue, P., Bernet, A., Mehlen, P. and Chédotal, A. (2017). Floor-plate-derived netrin-1 is dispensable for commissural axon guidance. *Nature* **545**, 350-354.

Fazeli, A., Dickinson, S. L., Hermiston, M. L., Tighe, R. V., Steen, R. G., Small, C. G., Stoeckli, E. T., Keino-Masu, K., Masu, M., Rayburn, H. et al. (1997). Phenotype of mice lacking functional Deleted in colorectal cancer (Dcc) gene. *Nature* **386**, 796-804.

Friedl, P. and Mayor, R. (2017). Tuning collective cell migration by cell–cell junction regulation. *Cold Spring Harb. Perspect. Biol.* **9**, a029199.

Friocourt, F. and Chédotal, A. (2017). The Robo3 receptor, a key player in the development, evolution, and function of commissural systems. *Dev. Neurobiol.* **77**, 876-890.

Garrett, A. M., Jucius, T. J., Sigaud, L. P. R., Tang, F.-L., Xiong, W.-C., Ackerman, S. L. and Burgess, R. W. (2016). Analysis of expression pattern and genetic deletion of netrin5 in the developing mouse. *Front. Mol. Neurosci.* **9**, 1-14.

Geisen, M. J., Meglio, T. D., Pasqualetti, M., Ducret, S., Brunet, J.-F., Chedotal, A. and Rijli, F. M. (2008). Hox paralog group 2 genes control the migration of mouse pontine neurons through slit-robo signaling. *PLoS Biol.* **6**, e142.

Harfe, B. D., Scherz, P. J., Nissim, S., Tian, H., McMahon, A. P. and Tabin, C. J. (2004). evidence for an expansion-based temporal Shh gradient in specifying vertebrate digit identities. *Cell* **118**, 517-528.

Kawauchi, D. (2006). Direct visualization of nucleogenesis by precerebellar neurons: involvement of ventricle-directed, radial fibre-associated migration. *Development* **133**, 1113-1123.

Keino-Masu, K., Masu, M., Hinck, L., Leonardo, E. D., Chan, S. S.-Y., Culotti, J. G. and Tessier-Lavigne, M. (1996). Deleted in colorectal cancer (DCC) encodes a netrin receptor. *Cell* **87**, 175-185.

Kennedy, T. E., Serafini, T., de la Torre, J. and Tessier-Lavigne, M. (1994). Netrins are diffusible chemotropic factors for commissural axons in the embryonic spinal cord. *Cell* **78**, 425-435.

Kim, D. and Ackerman, S. L. (2011). The UNC5C netrin receptor regulates dorsal guidance of mouse hindbrain axons. *J. Neurosci.* **31**, 2167-2179.

Kolodziej, P. A., Timpe, L. C., Mitchell, K. J., Fried, S. R., Goodman, C. S., Jan, L. Y. and Jan, Y. N. (1996). frazzled encodes a drosophila member of the DCC immunoglobulin subfamily and is required for CNS and motor axon guidance. *Cell* **87**, 197-204.

Kratochwil, C. F., Maheshwari, U. and Rijli, F. M. (2017). The long journey of pontine nuclei neurons: from rhombic lip to cortico-ponto-cerebellar circuitry. *Front. Neural Circuits* **11**, 1-19.

Krimpenfort, P., Song, J.-Y., Proost, N., Zevenhoven, J., Jonkers, J. and Berns, A. (2012). Deleted in colorectal carcinoma suppresses metastasis in p53-deficient mammary tumours. *Nature* **482**, 538-541.

Kucenas, S., Wang, W.-D., Knapik, E. W. and Appel, B. (2009). A selective glial barrier at motor axon exit points prevents oligodendrocyte migration from the spinal cord. *J. Neurosci.* **29**, 15187-15194.

Laumonnerie, C., Da Silva, R. V., Kania, A. and Wilson, S. I. (2014). Netrin 1 and Dcc signalling are required for confinement of central axons within the central nervous system. *Development* **141**, 594-603.

Li, W., Lee, J., Vikis, H. G., Lee, S.-H., Liu, G., Aurandt, J., Shen, T.-L., Fearon, E. R., Guan, J.-L., Han, M. et al. (2004). Activation of FAK and Src are receptor-proximal events required for netrin signaling. *Nat. Neurosci.* **7**, 1213-1221.

Marillat, V., Sabatier, C., Failli, V., Matsunaga, E., Sotelo, C., Tessier-Lavigne, M. and Chédotal, A. (2004). The slit receptor Rig-1/Robo3 controls midline crossing by hindbrain precerebellar neurons and axons. *Neuron* **43**, 69-79.

Mauti, O., Domanitskaya, E., Andermatt, I., Sadhu, R. and Stoeckli, E. T. (2007). Semaphorin6A acts as a gate keeper between the central and the peripheral nervous system. *Neural Dev.* **2**, 28.

Mehlen, P., Delloye-Bourgeois, C. and Chédotal, A. (2011). Novel roles for Slits and netrins: axon guidance cues as anticancer targets? *Nat. Rev. Cancer* **11**, 188-197.

Moore, S. W., Biais, N. and Sheetz, M. P. (2009). Traction on immobilized netrin-1 is sufficient to reorient axons. *Science* **325**, 166-166.

Nishitani, A. M., Ohta, S., Yung, A. R., del Rio, T., Gordon, M. I., Abraira, V. E., Avilés, E. C., Schoenwolf, G. C., Fekete, D. M. and Goodrich, L. V. (2017). Distinct functions for netrin 1 in chicken and murine semicircular canal morphogenesis. *Development* **144**, 3349-3360.

Pierce, E. T. (1966). Histogenesis of the nuclei griseum pontis, corporis pontobulbaris and reticularis tegmenti pontis (Bechterew) in the mouse. An autoradiographic study. *J. Comp. Neurol.* **126**, 219-254.

Sabatier, C., Plump, A. S., Le Ma, A. S., Brose, K., Tamada, A., Murakami, F., Lee, E. Y.-H. and Tessier-Lavigne, M. (2004). The divergent Robo family protein Rig-1/Robo3 is a negative regulator of slit responsiveness required for midline crossing by commissural axons. *Cell* **117**, 157-169.

Serafini, T., Kennedy, T. E., Gaiko, M. J., Mirzayan, C., Jessell, T. M. and Tessier-Lavigne, M. (1994). The netrins define a family of axon outgrowth-promoting proteins homologous to C. elegans UNC-6. *Cell* **78**, 409-424.

Serafini, T., Colamarino, S. A., Leonardo, E. D., Wang, H., Beddington, R., Skarnes, W. C. and Tessier-Lavigne, M. (1996). Netrin-1 is required for commissural axon guidance in the developing vertebrate nervous system. *Cell* **87**, 1001-1014.

Stanco, A. and Anton, E. S. (2013). Radial migration of neurons in the cerebral cortex. In *Cellular Migration and Formation of Neuronal Connections* (ed. J. L. R. Rubenstein and P. Rakic), pp. 317-330. Amsterdam, The Netherlands: Elsevier.

Suter, T. A. C. S., DeLoughery, Z. J. and Jaworski, A. (2017). Meninges-derived cues control axon guidance. *Dev. Biol.* **430**, 1-10.

Tronche, F., Kellendonk, C., Kretz, O., Gass, P., Anlag, K., Orban, P. C., Bock, R., Klein, R. and Schütz, G. (1999). Disruption of the glucocorticoid receptor gene in the nervous system results in reduced anxiety. *Nat. Genet.* **23**, 99-103.

Varadarajan, S. G., Kong, J. H., Phan, K. D., Kao, T.-J., Panaitof, S. C., Cardin, J., Eltzschig, H., Kania, A., Novitch, B. G. and Butler, S. J. (2017). Netrin1 produced by neural progenitors, not floor plate cells, is required for axon guidance in the spinal cord. *Neuron* **94**, 790-799.e3.

Vermeren, M., Maro, G. S., Bron, R., McGonnell, I. M., Charnay, P., Topilko, P. and Cohen, J. (2003). Integrity of developing spinal motor columns is regulated by neural crest derivatives at motor exit points. *Neuron* **37**, 403-415.

Voiculescu, O., Charnay, P. and Schneider-Maunoury, S. (2000). Expression pattern of a Krox20/Cre knock-in allele in the developing hindbrain, bones, and peripheral nervous system. *Genesis* **26**, 123-126.

Wullimann, M. (2011). The long adventurous journey of rhombic lip cells in jawed vertebrates: a comparative developmental analysis. *Front. Neuroanat.* **5**, 27.

Yee, K. T., Simon, H. H., Tessier-Lavigne, M. and O'Leary, D. D. M. (1999). Extension of long leading processes and neuronal migration in the mammalian brain directed by the chemoattractant netrin-1. *Neuron* **24**, 607-622.

Zelina, P., Blockus, H., Zagar, Y., Péres, A., Friocourt, F., Wu, Z., Rama, N., Fouquet, C., Hohenester, E., Tessier-Lavigne, M. et al. (2014). Signaling switch of the axon guidance receptor Robo3 during vertebrate evolution. *Neuron* **84**, 1258-1272.